Two Fast Transient Current Components during Voltage Clamp on Snail Neurons

ERWIN NEHER

From the Max-Planck-Institut für Psychiatrie, Munich, Germany

ABSTRACT Voltage clamp currents from medium sized ganglion cells of *Helix pomatia* have a fast transient outward current component in addition to the usually observed inward and outward currents. This component is inactivated at normal resting potential. The current, which is carried by K^+ ions, may surpass leakage currents by a factor of 100 after inactivation has been removed by hyperpolarizing conditioning pulses. Its kinetics are similar to those of the inward current, except that it has a longer time constant of inactivation. It has a threshold close to resting potential. This additional component is also present in giant cells, where however, it is less prominent. Pacemaker activity is controlled by this current. It was found that inward currents have a slow inactivating process in addition to a fast, Hodgkin-Huxley type inactivation. The time constants of the slow process are similar to those of slow outward current inactivation.

INTRODUCTION

Voltage clamp currents from nerve fibers have been given much attention and their properties have been described in detail (Hodgkin and Huxley, 1952; Frankenhaeuser and Huxley, 1964; Binstock and Goldman, 1969; Julian, Moore, and Goldman, 1962). Considering their very specialized task, propagation of impulses, it is not surprising that data obtained from them cannot explain more specialized phenomena, as for instance pacemaker activity (Guttman and Barnhill, 1970). Models for the simulation of nervous networks still have to rely on hypothetical modifications of the Hodgkin-Huxley axon for the description of somatic and dendritic areas (Lewis, 1968).

Voltage clamp currents from soma membrane have been measured with a variety of preparations (Araki and Terzuolo, 1962; Hagiwara and Saito, 1959; Chamberlain and Kerkut, 1967; Alving, 1969; Geduldig and Gruener, 1970). In most cases, however, current artifacts from cell processes, showing up as all-or-nothing inward transients, prescribe severe limits to their interpretation. Frank and Tauc (1964) described a method by which these artifacts can

be reduced. Stevens (1969) has isolated soma membrane currents by axonal ligation. Based upon the Frank and Tauc method, we developed a patch clamp method and applied it to different kinds of *Helix pomatia* ganglion cells (Neher and Lux, 1969, 1971). A detailed and quantitative description of two current components from somatic membrane patches will be given here.

METHODS

The voltage clamp design has been described in detail in a previous article (Neher and Lux, 1969). To summarize, clamp currents from a limited patch of soma membrane are measured by applying a conventional two-needle clamp (two intracellular microelectrodes) to the cell interior, and additionally placing a two-chambered semi-micropipette (50–100 μ diameter, Ringer-filled) on the exposed soma. The pipette interior is held close to ground potential by feedback control. When applying a voltage pulse to the cell interior, only those clamp currents which cross the patch of membrane covered by the pipette, can be measured in the current chamber of the pipette. Ordinarily, however, pipette internal resistance would be too high and current would tend to leak under the pipette rim. Through adjustment of the feedback amplification of the pipette clamp, the effective internal resistance of the pipette is set to a correct value; presence of the pipette, then, minimally disturbs the current field in the immediate neighborhood of the cell. In this case, the whole arrangement can be regarded as a balanced Wheatstone bridge: the series combination of both the effective pipette internal impedance and membrane impedance under the pipette as one branch of the bridge; and the extracellular impedance together with the impedance of the rest of the cell surface as the other branch (see Fig. 3 from Neher and Lux, 1969). Bridge balancing is achieved by observing pipette current variations during slight movements of the pipette to and from the cell soma. The diagonal impedance of the bridge (impedance between pipette interior and exterior) is thereby changed. This will lead to variations in the magnitude of a standard signal—for example the extracellular current due to an unclamped action potential—unless the bridge is balanced. Contrary to Strickholm's (1961) pipette measurements on the muscle cell surface, the potential inside the pipette is kept close to ground, thereby avoiding large leakage currents under the pipette rim.

For the intracellular clamp a loop gain between 5000 and 10,000 was used which resulted in a settling time (10–90 % full deflection) of about 50 μsec when applying a voltage pulse and measuring with the voltage control electrode. Capacitive transients in the pipette were smaller than 2–4 na, about 100 μsec after test pulse onset. The frequency response of the current-measuring device was reduced to 1 kc for better noise suppression in most experiments, however. On the other hand, transient capacitive currents in whole cell recordings persisted for several milliseconds (see Fig. 1 B). This slow component is probably due to electrotonic spread of capacitive current from remote parts of the axon. Inward current notches produced by the axon are greatly reduced as shown in Fig. 1 A.

Pipette The pipette used during the experiments described here had an inner diameter of 75 μ and a wall thickness of about 10 μ. For calculating current densities, pipette currents were divided by the area of a circular disc of 78 $\mu\phi$. With this

procedure, the curvature of the cell surface and also invaginations of the membrane into the pipette have been neglected. Therefore, absolute values given (current densities, specific conductances, specific capacity) are not very reliable, and, in fact may be appreciably lower. Since the same procedure has been applied to all measurements, relationships among them should be correct, however.

Preparation Experiments were performed with ganglion cells from *Helix pomatia*. The present work is based on analysis of data from approximately 40 cells (25 animals). The preparation was continuously perfused and the temperature was kept constant (±0.3°C) at values between 13 and 15°C. Only the cells from a cluster

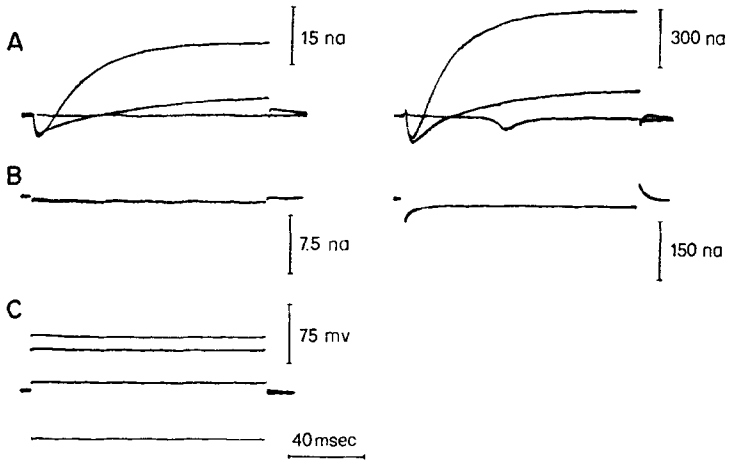

FIGURE 1. Comparison between pipette currents (left side) and simultaneously recorded whole cell currents (right side). A, superimposed currents corresponding to 12, 53, 72 mv depolarizing voltage pulses. Note late inward notch in the 12 mv trace, which is not present in the pipette recording. B, current due to a 60 mv hyperpolarizing voltage pulse at higher resolution. C, voltage traces common to both sets of current. Resting potential 45 mv; 14.5°C. Downward deflection represents inward current.

located at the entry of the anal nerve into the visceral ganglion (accessible from the ventral side of the suboesophageal mass) were used. The innermost connective tissue capsule can be opened in this area without much damage to the cell somas. This capsule must be opened to obtain adequate sealing of the pipette onto the cell membrane. The cell cluster contains one identifiable giant cell (diameter 200 μ), and 5–10 usable medium sized cells (100 $\mu < d < 200$ μ).

Solutions and Electrodes Physiological saline with the following composition (mM) was used: 95 NaCl; 4 KCl; 8 $CaCl_2$; 4 $MgCl_2$; 10 Tris; 10 maleic acid; 10 NaOH. Small quantities of NaOH were added to adjust the pH to 7.2–7.5. The electrodes for intracellular recording and current injection both contained 1.5 M K citrate and 1.5 M KCl mixed in a 10:1 ratio. They had outer tip diameters between 1 and 2 μ and impedances of 5–15 megΩ.

Clamp Current Analysis Pipette clamp currents were stored together with the voltage traces on magnetic tape. Later they were compared on the storage screen of

an oscilloscope with curves from a small analogue computer which had been programmed according to the Hodgkin-Huxley type equations (1, 2). Parameters of the computer curves were changed until the curves coincided with the experimental ones. The computer settings were then used to obtain values for curve parameters such as time constants, initial values, and absolute magnitudes.

RESULTS

The data obtained from membrane patches of snail nerve soma depend very much on resting potential. A set of clamp currents measured by starting from the natural resting potential of 45–55 mv resembles the squid currents with the difference that current densities are smaller and time courses are slower (Fig. 2, left column). Unlike squid axon, there is a relatively fast outward current inactivation (Frank and Tauc, 1964; Alving, 1969; Leicht, Meves, and Wellhörner, 1970; Neher and Lux, 1970, 1971; Geduldig and Gruener, 1970). Similar inactivation of outward currents has also been observed in many other preparations (see Grundfest, 1966).

If one starts from more hyperpolarizing holding potentials (60–80 mv), however, or if there are conditioning hyperpolarizing prepulses preceding the test pulses, currents observed are very different. Current traces from the center column of Fig. 2 are obtained in response to a series of voltage pulses which is identical to that of the left column; the only difference is a 45 mv hyperpolarizing prepulse of 500 msec duration preceding each test pulse. During the hyperpolarizing prepulses, there are only very small time-independent leakage currents. However, during test pulses which follow those prepulses, there are transient outward currents of appreciable amplitude even for clearly subthreshold voltages (first and second trace of the center column). First descriptions of this distinct current component are given by Stevens in *Archidoris* nerve cells (Stevens, 1969; Connor and Stevens, 1971 *a*, *b*) and, independently, by Neher and Lux (1970, 1971) in *Helix pomatia* neurons. The transients inactivate completely within 300–400 msec. For higher (superthreshold) voltage pulses, these currents are superimposed on the usually observed axon-like currents.

Simulation with an analogue computer showed that the clamp currents obtained in this way can always be represented as a mere additive superposition. Curve fitting was found to be simplest when there were two current curves available for one voltage level: one taken without a hyperpolarizing prepulse, and another with a prepulse to obtain maximal additional outward current. The parameters of the normal active currents can be determined with the first curve. When proceeding to the second curve, all the parameters concerning normal inward and outward currents remain the same. Absolute magnitude of the outward current has to be slightly readjusted, however, because of a different state of its inactivation after the prepulse. By subsequently

adjusting the settings for the fast transient component, a close fit is obtained. A set of current components simulated in this way is shown in the right column of Fig. 2.

The most prominent features of this additional current are its presence in the subthreshold voltage range, and its fast kinetics relative to the normal outward current. So far, all the observations concerning this current component can be described if one assumes it to be strictly additive to the usual clamp

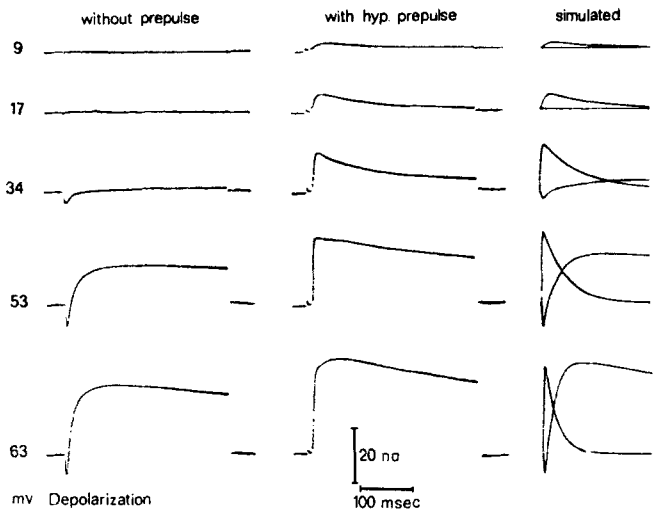

FIGURE 2. Left column, series of voltage clamp currents in response to depolarizing voltage pulses of magnitudes as indicated by numbers to the left (mv). Resting potential 48 mv; 14.5°C. Center column, 45 mv hyperpolarizing prepulses of 500 msec duration preceding test pulses. Test pulses are identical to those of left column. Note current artifacts which indicate ends of prepulses. During prepulses, there is a small inward going (downward) constant current. Right column, curves of center column split up through computer simulation into fast transient outward current component and normal inward plus outward components.

currents. At normal resting potentials it is almost completely inactivated unlike the partial inactivation of the Na^+ current in the Hodgkin-Huxley formulation. A hyperpolarizing prepulse removes this inactivation. Details of the inactivation curve, of time constants connected with activation and inactivation, and of the current-voltage characteristic will be presented in part II.

The observed current shapes suggest a quantitative description analogous to the Hodgkin-Huxley formulation with the modifications that there are: (*a*) an inactivation of the outward current; (*b*) an additional fast transient outward component I_A. The three active components are transient and are represented by products of activation and inactivation variables similar to the Hodgkin-Huxley Na^+ current. If the rectifier properties of the membrane

(Frankenhaeuser and Huxley, 1964) are included, the total current is:

$$\begin{aligned} I &= I_C + I_L + I_{in} + I_K + I_A \\ &= C\,dV/dt + g_L(V - V_L) + \bar{I}_{in}(V, V_{in})m^3h + \bar{I}_K(V, V_K)n^4k + \bar{I}_A(V, V_A)a^3b. \end{aligned} \tag{1}$$

For constant voltage V, the quantities a, b, m, h, n, and k are represented by

$$a(t, V) = a_\infty(V) + \{(a_0(V) - a_\infty(V)) \exp(-t/\tau_a(V))\} \tag{2}$$

and analogous expressions.
$\bar{I}_{in}(V, V_{in})$, $\bar{I}_K(V, V_K)$, and $\bar{I}_A(V, V_A)$ describe the instantaneous I-V relation for maximum activation according to

$$\bar{I}_K(V, V_K) = \bar{P}_K \cdot \frac{EF^2}{RT} \frac{[K]_0(1 - \exp\{(E - E_K)\cdot F/RT\})}{1 - \exp(EF/RT)}. \tag{3}$$

With the Hodgkin-Huxley formulation this expression is approximated by

$$\bar{I}_K(V, V_K) = \bar{g}_K(V - V_K). \tag{4}$$

Simulation on the analogue computer revealed that the clamp curves can be described by this set of equations within their experimental resolution, if only short clamp pulses (<300 msec) are given. The parameteric values obtained in this way will be presented in the following sections. More complicated phenomena occur with very long clamp pulses and during the time after termination of the clamp pulses (Neher and Lux, 1971). Therefore, a complete description of the normal outward currents has to be postponed until further analysis.

I. *Capacitive Currents and Leakage*

MEMBRANE CAPACITANCE This, was measured by determining the pipette current during application of a ramp-like voltage (Palti and Adelman, 1969) to the cell interior (Fig. 3). Nine measurements gave a value of 0.2 ± 0.04 nF for the patch of membrane under the pipette, or 4.1 [±0.8] μF/cm^2.

LEAKAGE CURRENTS These change linearly with voltage for hyperpolarizing voltage pulses from 20 to 80 mv magnitude (i.e. about −60 to −120 mv membrane voltage). In only a few cases were there indications of inward going rectification with hyperpolarizing voltage pulses of 60–80 mv. Conductances measured in the linear voltage range were 1.9 [±0.6]·10^{-4} Ω^{-1}/cm^2. In some cases leakage conductances as small as 1.1 × 10^{-4} Ω^{-1}/cm^2 were observed.

II. *Fast Transient Outward Currents*

As previously mentioned, there is an additional transient current component which is completely inactivated at normal resting potential. A 45 mv hyper-

polarizing conditioning pulse of 300–500 msec duration removes this inactivation. High resting potential (more than 55 mv) has a similar effect.

Once inactivation is removed, a series of voltage clamp pulses yields currents like those shown in Fig. 2 (center column). Current magnitude (i.e. current during the test pulse extrapolated to test pulse onset), plotted vs.

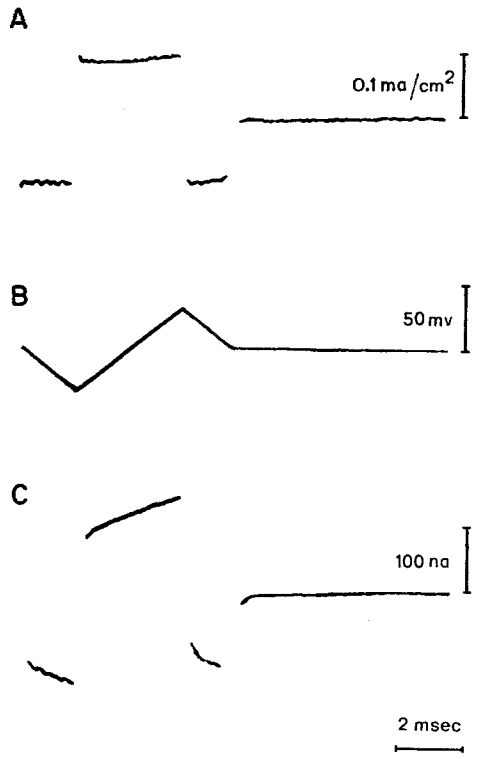

FIGURE 3. Determination of membrane capacitance. A, pipette currents in response to a voltage signal as shown in B. C, same as A, however with whole cell recording. 45 mv resting potential, 14.5°C. Capacitance C was measured according to $\Delta I = C\Delta(dU/dt)$, with ΔI being the pipette current difference between two points corresponding to the same, hyperpolarizing voltage.

membrane voltage, is shown in Fig. 4 A together with the corresponding quantities of the transient inward current and the normal K current. Existence of fast transient outward current in the voltage range below the appearance of transient inward current is obvious. On the other hand, it has a threshold of its own which is very close to resting potential. Fast outward transients as large as those from Fig. 4 A are regularly found in small or medium sized cells (100–200 μ ϕ). With giant cells, however, they very often are small or undetectable (Fig. 4 B).

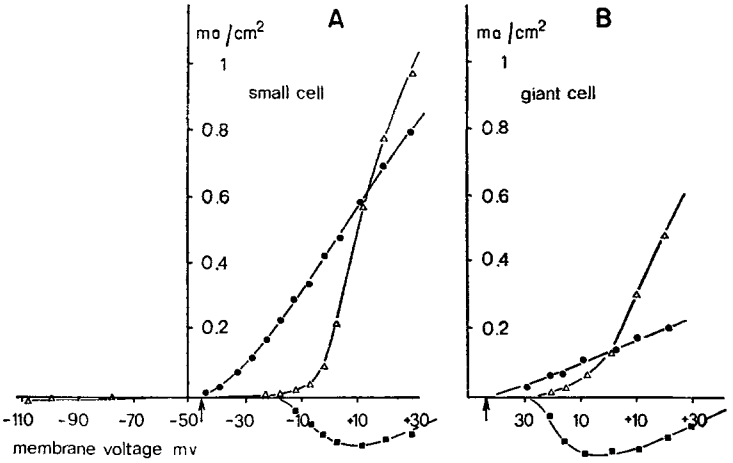

FIGURE 4. Current-voltage relations for a medium sized cell (A) and a giant cell (B) o fast transient outward current component (solid circles), normal outward component (open triangles), and normal inward component (solid squares). Total currents were split up by computer simulation as described in text. The values given are currents with their descending slopes extrapolated to the time of test pulse onset (the current that would be obtained if there was no inactivation). Resting potentials are indicated by arrows; 14–15°C. Outward current positive.

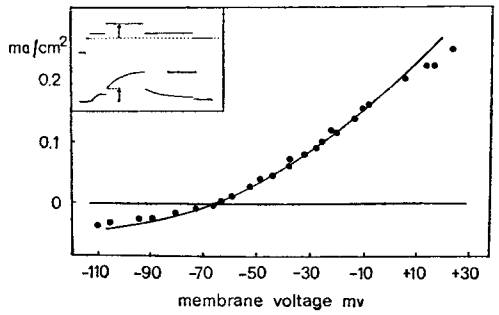

FIGURE 5. Instantaneous current-voltage relation during the peak of a pure fast transient outward current obtained as indicated in the insert. Values above −10 mv may include some inward current which is turning on very rapidly. According to the data presented it should be smaller 0.02 ma/cm². It may cause the deviations from the constant field curve (solid line). Cell from Fig. 4 A, same conditions. Insert, example of voltage and current forms used for obtaining the *I-V* relation. Dotted line indicates resting potential. Lengths of arrows indicate the quantities used for plotting. Time scale 40 msec.

Fig. 5 gives the instantaneous current-voltage relation of the fast transient outward current at its peak. This was obtained by producing a maximum pure response at a level of −28 mv, and then switching to a new voltage level. Current immediately after the switch is plotted vs. the new level. Typically

there is an outward going rectification according to the constant field equation. This was also observed in frog nodal membrane for the normal K current (Frankenhaeuser, 1962). The intersection of this curve with the voltage axis gives the equilibrium potential for the fast transient outward current. This potential is approximately 15–20 mv hyperpolarizing (around 65 mv membrane voltage). It is nearly identical with the equilibrium potential of the normal outward current (in the absence of the fast transient component) when measured at the end of a short superthreshold pulse. The latter potential, however, shifts to more positive values if there are large and longer lasting outward currents preceding the measurement (see also Alving, 1969).

If part of the external Na^+ is replaced by K^+, the equilibrium potentials of both the fast transient and the normal outward currents shift by the same amount. Neither value is influenced by the substitution of acetate for external Cl^-. These findings indicate strongly that the fast transient outward current component is carried by K^+. However, external concentrations of TEA which substantially alter the normal K currents (3–5 mM) do not affect the fast transient current.

The data from Figs. 4 A and 5 can be combined for determination of $\bar{P}_A$, V_A, and $a_\infty(V)$ from equations (2) and (3). V_A can be read directly from Fig. 5. Its value for the exemplar cell is -67 mv. The quantity $a^3_\infty(V)$ is obtained by dividing the fast transient currents $I_A(t_0, V)$ from Fig. 4 by the instantaneous currents $i_A(t_1, V)$ from Fig. 5 and normalizing, since this ratio is represented by:

$$\frac{I_A(t_0, V)}{i_A(t_1, V)} = \frac{a^3_\infty(V)b(t_0)\bar{I}_A(V, V_A)}{a^3(V_1, t_1)b(t_1)\bar{I}_A(V, V_A)} \propto a^3_\infty(V) \qquad (5)$$

V_1 voltage level before measurement.

$\bar{P}_A$ is determined from Fig. 5. After correction for incomplete activation and partial inactivation at the time of measurement, a value of $1.5 \cdot 10^{-4}$ (cm/sec) is obtained. This corresponds to a conductance g_A of $8.9 \cdot 10^{-3}\Omega^{-1}/\text{cm}^2$ if $I_A(V, V_A)$ is approximated by an expression of type (4). The mean value for $\bar{g}_A$ from nine medium sized cells was

$$7.6\ [\pm 1.7] \cdot 10^{-3}\Omega^{-1}/\text{cm}^2.$$

Dependence on Size and Duration of the Conditioning Pulse

Thus far behavior of the fast transient current has been described for a standard conditioning procedure (45 mv hyperpolarizing prepulse of 500 msec duration). Alternatively, test pulses can be maintained constant while size and duration of the prepulses are varied. A plot of peak current (normalized to 1 for maximum observed peak) vs. voltage level of the conditioning

pulse is given in Fig. 6 C (curve b_∞). This curve is analogous to the Na inactivation curve of Hodgkin and Huxley (1952). However, it is shifted on the voltage axis and is considerably steeper. The conditioning pulse was lengthened to guarantee a steady-state level of inactivation at its conclusion.

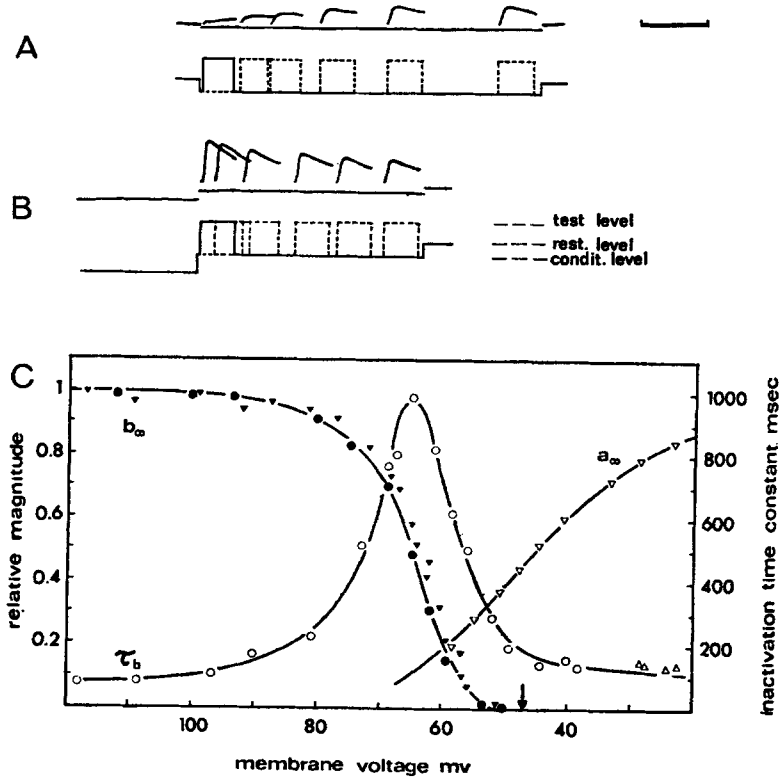

FIGURE 6. A, superimposed current traces in response to 20 mv test pulses (200 msec duration) at various times after the onset of a 15 mv hyperpolarizing conditioning pulse. Resting potential 50 mv, 13.5°C. Voltage traces drawn for clarity below. Traces superimposed graphically. Time scale, 400 msec. B, same as A, but more hyperpolarizing pulses are now preceding in every record. C, inactivation curve b_∞ (inverted solid triangles, same cell as that from Figs. 4 and 5; solid circles, different cell) together with the time constant τ_b measured as indicated in A and B. The steady-state value of the activation variable a_∞ (see text) is included for comparison with b_∞. Arrow indicates average resting potential. The half-value of the inactivation curve had an average of $-65[+1.5]$ mv over seven experiments.

For investigating the time courses of development and removal of inactivation, conditioning pulses are terminated at various times, and test pulses applied immediately afterwards (Fig. 6 A). Current peaks during the test level are plotted vs. duration of the conditioning pulse. With longer duration, the current peaks increase towards a steady-state value (depending on con-

ditioning level) which is given by the inactivation curve of Fig. 6 C. The increase is almost exponential, although it seems sometimes that the beginning has a sigmoid shape. The latter observation was not considered in the mathematical description. The time constants, as derived from exponential plots, are functions of the conditioning level (Fig. 6 C, curve τ_b).

For conditioning voltage levels corresponding to about half-inactivation (65 mv), two alternative experiments of this type can be performed: one, as described above (Fig. 6 A), and another one with additional more hyperpolarizing pulses preceding the conditioning pulses (Fig. 6 B). In this case, a maximal current peak is observed if the conditioning level is terminated early enough. With increasing duration of the conditioning pulse, current peaks decay exponentially towards the same steady-state level, and with the same time constant as previously.

As shown below, steady-state values and time constants measured by these methods are the quantities b_∞ and τ_b of expression (2). If the descending slopes of the currents were extrapolated towards time of onset of the test pulse (t_0), one would measure a quantity $I(t_0)$:

$$I(t_0) = a_\infty^3(V_{\text{test}}) \cdot b(t_0) \bar{I}_A(V_{\text{test}}, V_A).$$

Since the test level V_{test} does not change, all values are constant except $b(t_0)$. $I(t_0)$ is therefore proportional to $b(t_0)$. Peaks of currents will be proportional to $I(t_0)$, since for constant test voltage they occur at fixed times after test pulse onsets. This holds, except for depolarizing conditioning levels, which cause slight activation of the variable a during conditioning.

KINETICS A pure fast transient outward response which can be activated in the range from -45 to -30 mv transmembrane voltage shows a sigmoid rising phase and an exponential decay (Fig. 7). With more depolarization it is superimposed by the normal inward and outward currents. The rising phase can be fitted reasonably well by an exponential raised to a power of at least three to four. It is difficult, however, to determine the exact value. A power of three was chosen for ease of comparison with the Hodgkin-Huxley equations for the Na current. Under this assumption the time constant of this rise(τ_a) can be determined from curves of Fig. 7 for membrane voltages between -45 to -30 mv (Fig. 8, τ_a). For higher depolarizing voltages the normal active currents are subtracted, and time constants determined by computer simulation. The curve is extended to more hyperpolarizing voltage levels by simulating the current tails observed when the membrane is repolarized to different levels at the time of peak currents.

Inactivation of the fast transient outward current is strictly exponential and complete for all detectable current variations in the subthreshold voltage range. There is some ambiguity about the completeness of this inactivation

with more depolarizing voltages since a small steady-state component cannot be easily detected in the presence of large normal outward currents. Complete inactivation has been assumed for all evaluations. Time constant

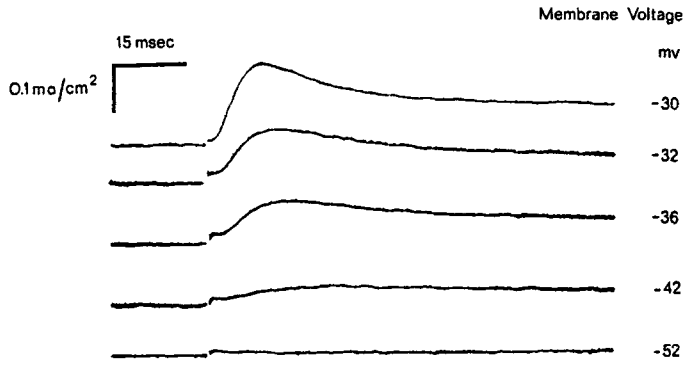

FIGURE 7. Fast transient outward currents in response to a voltage step from a −95 mv hyperpolarizing conditioning level to the test levels indicated on the right (mv). Uppermost curve contains some normal outward current which is very slowly turning on, and also some very small inward current which shifts the beginning of the curve slightly downward. Resting potential 51 mv; 13.5°C.

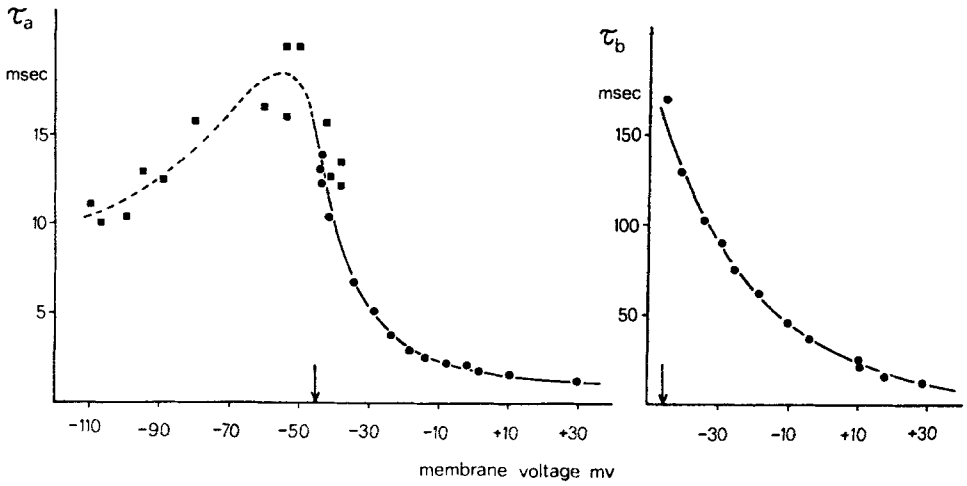

FIGURE 8. Time constants of rise (τ_a) and fall (τ_b) of the fast transient outward current from cell of Figs. 4 and 5. (Solid circles), τ_a values obtained from simultation of current rise. (Solid squares), τ_a values obtained by analyzing tails.

of inactivation (τ_b) is plotted vs. transmembrane voltage in Fig. 8. The curve can be extended to hyperpolarizing potentials by the values for τ_b, given in Fig. 6 C.

When temperature was varied between 10 and 22°C the time constant of

inactivation was found to be considerably less temperature-dependent ($Q_{10} \sim$ 2.4) than the time constant of activation which showed a Q_{10} of approximately 3.

Combining τ_a and τ_b from Fig. 8 with the values for a_∞ and b_∞ from Fig. 6 C allows the rate constants α_a, β_a, α_b, β_b to be calculated.

III. *Transient Inward Currents*

The same method of analysis presented for the fast transient outward component can be undertaken for the transient inward current. However, these measurements are considerably less precise because transient inward currents: (*a*) are superimposed on a larger outward current under most conditions, (*b*) are smaller in magnitude, and (*c*) have a faster time course (Fig. 9).

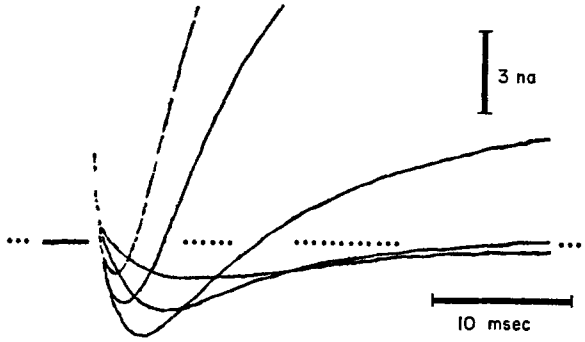

FIGURE 9. Clamp currents at higher time resolution for 32, 39, 53, 71, and 81 mv depolarizing test pulses. 40 mv resting potential, 12°C.

CURRENT VOLTAGE RELATION Two typical *I-V* plots from cells with average inward current are given in Fig. 4. However, absolute magnitudes of inward currents vary greatly from cell to cell. In some cases there was a steady decrease of inward current during longer periods of registration from one cell. This observation (aging effect) has no counterpart in outward currents.

The equilibrium potential of the inward current was found to be between +50 and +60 mv. In order to determine its conductance $\bar{g}_{in}$, the limiting (depolarizing) slopes from *I-V* plots like those in Fig. 4 are corrected for inactivation at the resting potential (see below). Eight measurements yield a value of 9 $[\pm 3.7] \cdot 10^{-3}\ \Omega^{-1}/\text{cm}^2$. The inactivation curve $h_\infty(V)$ can be determined in the same way as the one for the fast transient outward current (Fig. 10). However, the onset of the fast transient K^+ current will usually distort the curve in the hyperpolarizing range (around −55 mv). In order to normalize the inactivation curve, the value of 0.5 was given to the point of steepest slope of the plot.

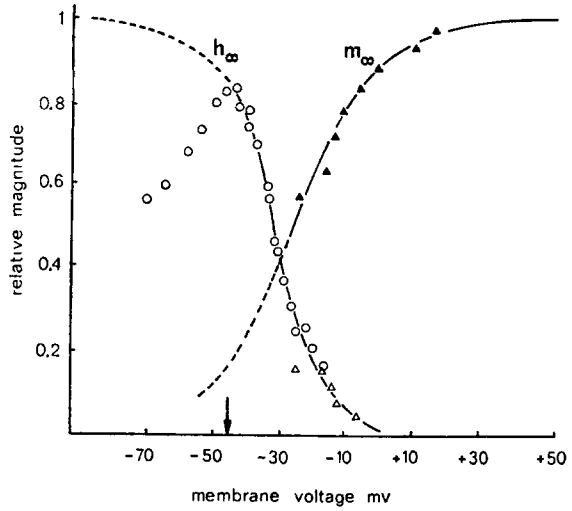

FIGURE 10. Variables of activation (m_∞) and inactivation (h_∞) of the inward current as a function of membrane voltage. Values for h_∞, represented by open circles, were obtained in the manner illustrated in Fig. 6 A. The other values originate from computer simulations. Arrow indicates resting potential, 13°C.

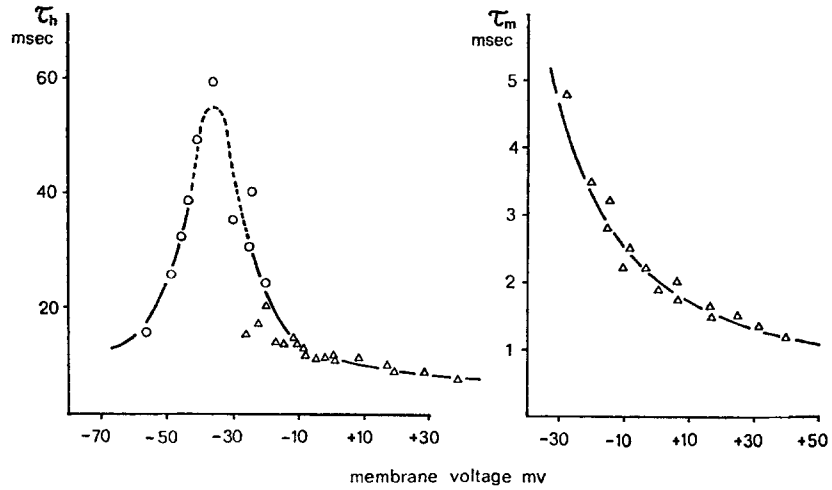

FIGURE 11. Time constants of activation and inactivation of the inward current. Meaning of symbols analogous to Fig. 10, 13°C. Data represented by triangles are pooled from three cells.

KINETICS Time constants of activation and inactivation (Fig. 11) can be determined by the simulation of curves like those from Fig. 9. Analogous to curve τ_b the curve for τ_h can be extended to more negative values of potential. The experiments show clearly that there is a peak of τ_h around −35 mv. But, only a rough estimate of its maximum value can be given. It

should be noted that measurement of the parameters $\bar{g}_{in}$, τ_m, and τ_h is influenced by the choice of parameters for the outward current. It is n_0, the initial value of the outward current, which has the greatest influence on initial parts of the slope. A value for n_0 of 0.25 was found useful, and taken as a standard. It was also found helpful to determine the ratio $\tau_m:\tau_h$ from traces with maximum inward current, and to adopt this ratio as a constant for traces corresponding to more depolarizing voltages. This seems to be justified from voltage clamp data on other preparations.

In addition to the inactivation of the inward current described above there is a second, slow component of inactivation. When applying two short voltage pulses of about 10 msec duration and with a pulse interval of 120 msec (larger than the time required for removal of inactivation as described above), the inward current of the second pulse is almost as large as that of the first pulse. For constant pulse intervals, the test inward current decreases, however, when the first pulse is of a longer duration. The decrease almost parallels the slow outward current inactivation. With an 80 msec duration for the first pulse, it is decreased to half; and with a 400 msec duration, there is essentially no inward current. Recovery from this inactivation is extremely slow (about 1 sec for half-recovery at 13°C).

A slow inactivation process of inward current has been described by Chandler and Meves (1970) in squid axon. Adelman and Palti (1969) also described long-term inactivation of Na^+ conductance in squid axon due to increased extracellular K^+ concentration. It seems possible that this process is caused by K^+ accumulation during longer pulses in a restricted extracellular space (Frankenhaeuser-Hodgkin space).

DISCUSSION

Voltage clamp currents from limited patches of *Helix pomatia* soma surface differ from squid axon currents in that they are slower and smaller in magnitude. Contrary to squid, late outward conductivity dominates transient inward conductivity (see also Neher and Lux, 1971). This may explain the observation that unclamped membrane patches were always driven from other parts of the cell. During the rising phase of an action potential there are net outward currents registered in the pipette, even in the case of spontaneously firing cells not yet penetrated by intracellular microelectrodes. Thus, the soma seems to be predominantly a source of hyperpolarizing currents. This point is also stressed by the existence of a fast transient outward current. Whenever the cell hyperpolarizes more than approximately 50 mv (spike afterhyperpolarization, high resting potential, hyperpolarizing IPSP), its behavior upon return to normal resting potential is controlled by this current. The action of the fast transient current lasts for some 200–400 msec, until it is finally inactivated, and has the tendency to prolong polarization.

As Connor and Stevens (1971 *c*) have shown, the typical repetitive firing behavior of snail neurons under the action of a wide range of constant driving currents can be predicted if the fast transient outward current is considered in computations. Once a spike is triggered, spike afterhyperpolarization will partly remove inactivation. Thereupon transient outward current will counteract the driving current until it is again inactivated. In this way the refractory period can be overcome, and a new spike will be triggered after an interval which is strongly dependent on the inactivation time constant of the fast transient outward current.

The fast transient outward current has a striking similarity to the other active current components. It has a threshold of its own, an inactivation curve similar to that of the inward current, and an instantaneous current-voltage relation according to the independence principle. The possibility that it might be caused by activation of normal active currents in a neighborhood of lower threshold (axon hillock) is ruled out as follows: a positive going prepulse applied to the pipette has the same effect as a hyperpolarizing one applied to the cell interior. In the first case, conditioning action is restricted to just the membrane patch under the pipette.

Fast transient outward currents are very well-suited for the study of electrically induced permeability changes. Their advantages over the other current components are: (*a*) They can be observed, uncontaminated by other components, over a large voltage range; other active and leakage currents going along with them are smaller, often by a factor of 50–100, (*b*) they are relatively slow, so that response time of the voltage clamp system is a minor problem, (*c*) they are small enough to guarantee a very good space clamp over the entire area under investigation.

An interesting point in this respect is the steepness and the excellent reproducibility of the inactivation curve b_∞ (Fig. 6 C). When it is fitted by

$$b_\infty = 1/[1 + \exp((E - E_b)/a)]$$

the quantities a and E_b are determined as 4 [$\pm$0.5] mv and 65 [$\pm$1.5] mv, respectively. The quantity a for Na inactivation in squid is 7 mv (Hodgkin and Huxley, 1952).

Inward Current It was shown by Geduldig and Gruener (1970) that inward current in *Aplysia* is carried by both Na^+ and Ca^{++} ions. They also found an abnormality in the inactivation curve of the Ca^{++} component. The inactivation variable had a maximum around 60 mv and decreased for more hyperpolarizing values. In the investigation described here a similar phenomenon was observed. Geduldig and Gruener interpret this behavior as a new mechanism of inactivation. According to the results presented here, it seems more likely that the abnormality is due to the fast transient outward

current. In giant cells transient outward currents are often very small. During whole cell recordings, they are easily overlooked, since they are masked by inward notches in subthreshold voltage range. The transient outward currents counteract inward currents, however, if test pulses are preceded by hyperpolarizing conditioning pulses. The fact that the abnormality is observed only in the Ca^{++} component may be due to the slow time course of the latter. With the Na^{+} component, inward peaks may develop so early that the fast transient potassium component has not yet fully turned on at the time of peak. A test for this alternative explanation of Geduldig and Gruener's findings would be to measure membrane conductivity and equilibrium potential at the time of peak inward current.

I would like to thank Dr. H. D. Lux for his consistent help during this work.
I am also indebted to Dr. C. F. Stevens for supplying me with preprints of his recent work.

Received for publication 12 February 1971.

BIBLIOGRAPHY

ADELMAN, W. J., JR., and Y, PALTI. 1969. The effects of external potassium and long duration voltage conditioning on the amplitude of sodium currents in the giant axon of the squid. *Loligo peali. J. Gen. Physiol.* **54**:589.

ALVING, B. O. 1969. Differences between pacemaker and nonpacemaker neurons of *Aplysia* on voltage clamping. *J. Gen. Physiol.* **54**:512.

ARAKI, T., and C. A. TERZUOLO. 1962. Membrane currents in spinal motoneurons associated with the action potential and synaptic activity. *J. Neurophysiol.* **25**:772.

BINSTOCK, L., and L. GOLDMAN. 1969. Current- and voltage-clamped studies on *Myxicola* giant axons. Effect of tetrodotoxin. *J. Gen. Physiol.* **54**:730.

CHAMBERLAIN, S. G., and G. A. KERKUT. 1967. Voltage clamp studies on snail (Helix aspersa) neurones. *Nature* (*London*). **216**:89.

CHANDLER, W. K., and H. MEVES. 1970. Slow changes in membrane permeability and long lasting action potentials in axons perfused with fluoride solutions. *J. Physiol.* (*London*). **211**:707.

CONNOR, J. A., and C. F. STEVENS. 1971 *a*. Inward and delayed outward membrane currents in isolated neural somata under voltage clamp. *J. Physiol.* (*London*). **213**:1.

CONNOR, J. A., and C. F. STEVENS. 1971 *b*. Voltage clamp studies of a transient outward membrane current in gastropod neural somata. *J. Physiol.* (*London*). **213**:21.

CONNOR, J. A., and C. F. STEVENS. 1971 *c*. Prediction of repetitive firing behaviour from voltage clamp data on an isolated neurone soma. *J. Physiol.* (*London*). **213**:31.

FRANK, K., and L. TAUC. 1964. Voltage clamp studies of molluscan neuron membrane properties. *In* The Cellular Function of Membrane Transport. J. Hoffmann, editor. Englewood Cliffs, N.J., Prentice-Hall, Inc. 113.

FRANKENHAEUSER B. 1962. Potassium permeability in myelinated nerve fibres of Xenopus laevis. *J. Physiol* (*London*). **160**:54.

FRANKENHAEUSER, B., and A. F. HUXLEY. 1964. The action potential in the myelinated nerve fibre of Xenopus laevis as computed on the basis of voltage clamp data. *J. Physiol.* (*London*). **171**:302.

GEDULDIG, D., and R. GRUENER. 1970. Voltage clamp on the Aplysia giant neurone: Early sodium and calcium currents. *J. Physiol.* (*London*). **211**:217.

GRUNDFEST, H. 1966. Comparative electrobiology of excitable membranes. *Advan. Comp. Physiol. Biochem.* **55**:104.

GUTTMAN, R., and R. BARNHILL. 1970. Oscillation and repetitive firing in squid giant axons. *J. Gen. Physiol.* **55**:104.

HAGIWARA, S., and N. SAITO. 1959. Voltage-current relation in nerve cell membrane of Onchidium verruculatum. *J. Physiol. (London).* **148**:161.

HODGKIN, A. L., and A. F. HUXLEY. 1952. A quantitative description of membrane current and its application to conduction and excitation in nerve. *J. Physiol. (London).* **117**:500.

JULIAN, F. J., J. W. MOORE, and D. E. GOLDMAN. 1962. Current-voltage relations in the lobster giant axon membrane under voltage clamp conditions. *J. Gen. Physiol.* **45**:1217.

LEICHT, R., H. MEVES, and H. WELLHÖRNER. 1970. Voltage-Clamp-Versuche an Riesennervenzellen der Weinbergschnecke Helix pomatia. *Pfluegers Arch. Ges. Physiol. Menschen Tierre.* **316**:R66.

LEWIS, E. R. 1968. Using electronic circuits to model simple neuroelectric interactions. *Proc. IEEE.* **56**:931.

NEHER, E., and H. D. LUX. 1969. Voltage clamp on Helix pomatia neuronal membrane; current measurement over a limited area of the soma surface. *Pfluegers Arch. Ges. Physiol. Menschen Tiere.* **311**:272.

NEHER, E., and H. D. LUX. 1970. Abweichungen vom Hodgkin-Huxley-Formalismus bei Voltage Clamp Versuchen an Helix pomatia. *Pfluegers Arch. Ges. Physiol. Menschen Tiere.* **319**:R107.

NEHER, E., and H. D. LUX. 1971. Properties of somatic membrane patches of snail neurons under voltage clamp. *Pfluegers Arch. Ges. Physiol. Menschen Tiere.* **322**:35.

PALTI, Y., and W. J. ADELMAN, JR. 1969. Measurement of axonal membrane conductances and capacity by means of a varying potential control voltage clamp. *J. Membrane Biol.* **1**:431.

STEVENS, C. F. 1969. Voltage clamp analysis of a repetitively firing neuron. *In* Basic Mechanisms of the Epilepsies. H. H. Jaspers, A. A. Ward, and A. Pope, editors. Little, Brown and Company, Inc., Boston, Mass. 76.

STRICKHOLM, A. 1961. Impedance of a small electrically isolated area of the muscle cell surface. *J. Gen. Physiol.* **44**:1073.